Indian Journal of Pure & Applied Physics
Vol. 47, November 2009, pp. 775-781

Luminescence efficiency of Eu^{+3} in Y_2O_3: The effect of reduction of particle size and incorporation of trace hetero-cations in the Y_2O_3 lattice

A Nayak, K Goswami[1], A Ghosh & R Debnath*

Central Glass and Ceramic Research Institute, 196, Raja S C Mullick Road, Kolkata 700 032

[1]Department of Physics, Jadavpur University, Kolkata-700 032

E-mail: debnath@cgcri.res.in

Received 12 December 2008; revised 28 April 2009; accepted 26 August 2009

The effect of incorporation of trace (Al^{+3}, B^{+3}) in the Y_2O_3 lattice on the luminescence efficiency of Y_2O_3:Eu^{+3} red phosphor has been investigated. It is observed that such incorporation causes an enhancement of $^5D_0 \rightarrow {}^7F_2$ red luminescence efficiency as well as the associated excitation efficiency of Eu^{+3}. It is concluded that there occurs a change in the polarity of the host rather than the site symmetry of Eu^{+3} due to incorporation of the hetero cations. Calculation of the Judd-Ofelt parameters gives similar results. In another study, to observe the effect of reduction of particle size on the luminescence efficiency of the Y_2O_3:Eu^{+3}, the change in luminescence efficiency of the phosphor with the reduction particle size and the stability of the different efficiencies with the elapse of time have been investigated. The samples with particle size below 100 nm showed a significant loss in luminescence efficiency and a change in their excitation profile with time. IR studies showed that although the freshly prepared samples were almost free from contaminated water, on ageing in air at room temperature, they absorb the latter. A phenomenon of hydration induced coupling of the excitonic state of Y_2O_3 with one of its F_u modes, has been detected in the case of the aged samples which susequently introduces newer non-radiative channels in the system causing a decrease in the luminescence efficiency of the phosphor. Because of larger surface to volume ratio, the effect is most pronounced in nanocrystalline samples.

Keywords:Y_2O_3:Eu^{+3} red phosphor, Luminescence efficiency, Host's polarity, Nanocrystals, Hydration, Non-radiative loss

1 Introduction

Eu^{+3} ions activated cubic Y_2O_3 is one of the most important commercial red phosphors used in lighting, plasma display panel (PDP), field emission display (FED), thermal calibration etc. Phosphors of lower particle size with higher luminescence efficiency are the most desired materials for use in compact fluorescent lamps of higher lumen power and display panels of better image-resolution. Amongst the various techniques[1-17] explored to improve the luminescence efficiency of a phosphor, the methods of (1) modification of structure of the host's lattice by introducing hetero cations[1,2,7-9] and (2) enhancement of the surface area of the phosphor by decreasing its particle size[3-6,10-16], are most familiar. In case of Y_2O_3:Eu^{+3}, although there are reports of both failure and success of application of the first method, result of application of the second method remained until recently a mystery.

In the context of the first approach for enhancement of luminescence efficiency mentioned above, we report that a significant enhancement of luminescence efficiency of Y_2O_3:Eu^{+3} phosphor can be achieved on introduction of trace Al^{+3} and B^{+3} ions in its host's lattice and argue that it occurs due to the change in the field strength of the host; while in connection with the second approach we revisited the problem of 'the effect of reduction of particle size on the luminescence efficiency' of the phosphor and deciphered that on storing the material in air, there occurred a phenomenon of hydration induced coupling of the excitonic state of Y_2O_3 with one of its F_u modes. In the case of nanocrystallite Y_2O_3:Eu^{+3}, the effect was most dominant and hence introduced huge non-radiative channels in the system causing a significant loss in luminescence efficiency.

2 Experimental Details

The phosphor samples of the first study were prepared by conventional solid state combustion reaction of a mixture of oxalates of the yttrium and europium in the composition (gram ion % Y^{+3} = 96.25, Eu^{+3} = 3.00), one with and the other without the addition of oxides of boron and aluminium (gram ion % B^{+3} = 0.150 and Al^{+3} = 0.600) at 1350°C for two hours. All the chemicals used were of GR grade

(Aldrich, E Merck). Phosphor samples of different sizes of the second study were prepared by similar solid-state combustion reaction of the mixed oxalates of the respective cations in a composition of Y^{+3} = 97.00 %, Eu^{+3} = 3.00% (gram ion) with or without the addition of 25-75 wt% of powdered glycine (all chemicals were of E Merck, GR grade). They were stored in air at room temperature for ageing.

The X-ray powder diffraction spectra were recorded in a diffractometer (model: PW1710 BASED, make:Philips) using a copper anode. A Field Emission Scanning Electron Microscope (FESEM) was used to record the micrographs of the samples. The emission and excitation spectra were recorded in a Perkin Elmer LS55 Spectrofluorimeter. The quantitative luminescence and excitation spectra of the samples under 254 nm excitation, were recorded at room temperature using front surface illumination technique taking each time a fixed quantity of the material packed in a groove of definite volume (cross-sectional diameter = 0.50 mm) on a brass plate and keeping the emission and excitation slits as well as the lamp condition the same. To avoid any detrimental effect of ageing on the luminescence efficiency of the samples of the first study, the emission spectra of the samples were recorded within 2-3 days of their preparation. The lifetime of the $^5D_0$ luminescence state of Eu^{+3} ions of each sample was recorded in a luminescence lifetime measurement set up (model:Fluorocube, IBH, UK) using multichannel analyzer technique. A spectra-LED (IBH) emitting at 372 nm with pulse duration of 100 microseconds and operating at a repetition rate of 40 Hz was used as the excitation source.

3 Results and Discussion

3.1. Effect of incorporation of Al^{+3} and B^{+3} in the host's lattice

The phase purity of the Y_2O_3:Eu^{+3} phosphor and that of its (Al^{+3}, B^{+3}) containing counter part was checked by X-ray diffraction study. The diffraction patterns of both the samples were identical and conformed[18] to that of cubic phase of yttria (Fig. 1). The result showed that the incorporation of trace B^{+3} and Al^{+3} ions (0.150 and 0.600, g ion %, respectively) in the Y_2O_3 lattice did not induce any change in the cubic structure of the latter. The crystallite size of each of the samples was calculated from the half-width of the (222) diffraction line of the sample using the Scherrer equation $d = 0.92\{\lambda/(\beta_{1/2}\times\cos\theta)\}$, where d is the diameter of the crystallite, λ the wavelength of the X-ray, $\beta_{1/2}$ the line width at half maximum (in radian) and θ is the peak angle of the diffraction line. The calculated crystallite sizes were in the range 30-35 nm. It is, therefore, expected that there should not be much difference in the luminescence efficiency of the two samples due to difference in their particle size.

The $^5D_0 \rightarrow {}^7F_2$ quantitative luminescence spectra of the pure Y_2O_3:Eu^{+3} and that of (Al^{+3}, B^{+3}) containing sample under 254 nm excitation are shown in Fig. 2. The luminescence efficiency of the (B^{+3}, Al^{+3}) containing sample is found to be much higher than that of the pure sample. The consistency of the phenomenon was verified with different set of such

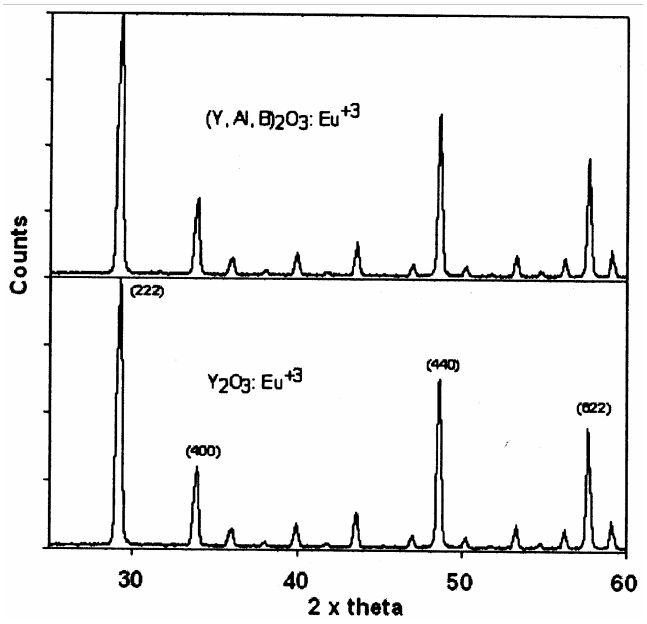

Fig. 1 — XRD spectra of pure Y_2O_3:Eu^{+3} and that of its (Al^{+3}, B^{+3}) containing counter part

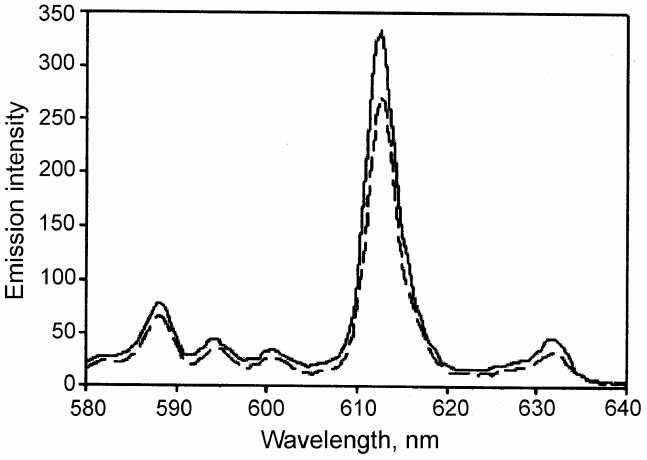

Fig. 2 — Quantitative luminescence spectra of the sample with Al^{+3} and B^{+3} as additional impurities (——) vis-à-vis that of the pure sample (------)

phosphors. The ratio of the integrated luminescence efficiency of the two samples (impure:pure = 3738.33/2920.76 = 1.28), shows that the luminescence efficiency of the (B^{+3}, Al^{+3}) containing sample is almost 1.28 times higher than that of the pure sample. Higher luminescence efficiency means higher emission rate [A (aJ; bJ′)] which in turn, is related to Judd Ofelt parameters (Ω_t) of the activator ion in the matrix[19,20]. Apparently, there may be two reasons for such enhancement of luminescence efficiency:(1) Change in the symmetry of the oxygen coordination surrounding the Eu^{+3} ions, (2) Change in the crystal field strength of the oxygen coordination due to the presence of relatively smaller Al^{+3} and B^{+3} cations in the lattice of yttria. The emission spectrum of the Eu^{+3} ions is known to be hypersensitive to the symmetry of its coordination structure and the slightest variation in its coordination symmetry causes a significant change in the pattern of its luminescence spectrum. In the present case, however, we do not find any change in the spectral pattern due to incorporation of Al^{+3} and B^{+3} ions in the lattice, so we can assume that there has not been any change in the symmetry of the oxygen coordination surrounding the Eu^{+3} ions as a result of incorporation of Al^{+3} and B^{+3} ions. Plausible reason of enhancement of luminescence efficiency in the case of (Al^{+3}, B^{+3}) containing phosphor therefore, seems to be a change in the field strength surrounding the Eu^{+3} ions. Considering the fact that the ionic sizes of Al^{+3} (0.50 Å) and B^{+3} (0.2 Å) are very small compared to that of Y^{+3} (0.93 Å) and as a consequence, a change in distribution of charge density over the oxygen coordination surrounding the Eu^{+3} ions may result. And consequently a change in the field-strength surrounding the Eu^{+3} ions, in the case of (Al^{+3}, B^{+3}) containing sample, is expected.

Figure 3 shows corresponding quantitative excitation spectra of the 612 nm ($^5D_0 \rightarrow {}^7F_2$) red emission of the two samples. Comparison of the excitation profile of the two samples shows that although the excitation conversion efficiency of the two samples is almost similar around the excitonic band of yttria (around 212 nm), the same is considerably higher along the (Eu^{+3}-O^{-2}) C-T band region (i.e. 220-280 nm region) in the case of (Al^{+3}, B^{+3}) containing sample. The oscillator strength of a charge transfer band is known to be greatly influenced by the polarizability of the medium. The observed enhancement of the excitation spectrum along the (Eu^{+3}-O^{-2}) C-T band region in the case of (Al^{+3}, B^{+3}) containing sample may, therefore, be the result of change in the polarizability or in other words, change in the charge distribution in the system.

The decays of the $^5D_0$ emitting state of Eu^{+3} in the case of the two samples are shown in Fig. 4. In case of the pure sample the decay is single exponential and shows a life time (T) of the order of 1.07×10^{-3} s. In case of (Al^{+3}, B^{+3}) containing sample, the decay profile shows bi-exponential feature, which consists of a faster component of $T_1 = 0.61\times10^{-3}$ s and a slower component of $T_2 = 1.05\times10^{-3}$ s. The slower component of the decay of the (Al^{+3}, B^{+3}) containing sample is, in fact, similar to that of the pure sample. The result suggests that there exist two different types of C_2 sites for Eu^{+3} ions in case of (Al^{+3}, B^{+3}) containing sample. The ions which correspond to the slower component of the $^5D_0$-decay have field structure identical to that of Eu^{+3} ions in C_2 sites of pure cubic yttria while the Eu^{+3} ions corresponding to

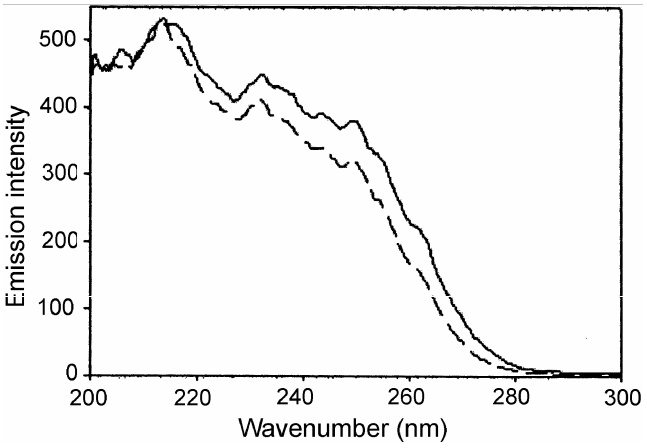

Fig. 3—Quantitative excitation spectra of the $^5D_0 \rightarrow {}^7F_2$ emission (λ_m = 612 nm) of the sample with Al^{+3} and B^{+3} as additional impurities (——), vis-à-vis that of the pure sample (------)

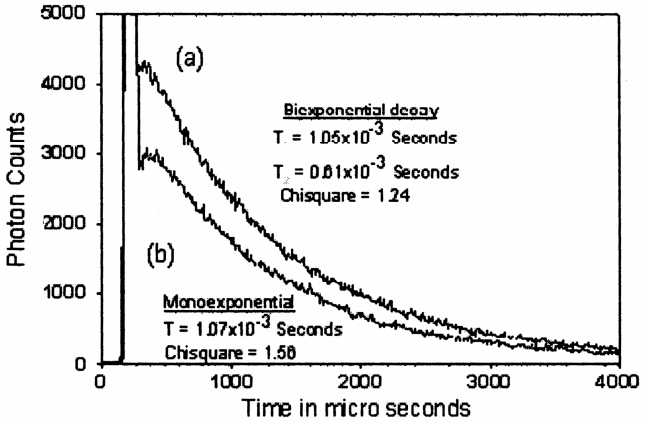

Fig. 4—Decay of the $^5D_0$ emitting state of Eu^{+3}:(a), the (Al^{+3}, B^{+3}) containing sample; (b), the pure sample

the faster component of the $^5D_0$-decay have oxygen coordination structure which have Al^{+3}/B^{+3} cation or both as the nearest neighbour. These neighbouring smaller cations can actually bring about a change in the charge distribution on the oxygen ions surrounding the Eu^{+3} ions of these sites forcing the emission to occur at a faster rate.

To cross-check the observed phenomenon of impurity ions induced change of the crystal field strength surrounding the Eu^{+3} ions, we have calculated the Judd-Ofelt[19,20] parameter (Ω_2) of the $^5D_0 \rightarrow {}^7F_2$ transition corresponding to those Eu^{+3} which have Al^{+3}/B^{+3} or both as the nearest neighbour, using the experimental decay times of Eu^{+3} of the pure and the impure sites (1.07×10^{-3} and 0.61×10^{-3} s, respectively) and the expression given in Eq. (1) for emission rate[21,24] of an electronic transition.

$$\text{Inverse of decay time } (T^{-1}) = A\,(aJ;bJ') = 64\pi^4(\nu)^3/3h(2J+1) * n(n^2+2)^2/ \times 9\, e^2 \sum_{t=2,4,6} \Omega_t \left| \langle (S,L)J \| U^{(t)} \| (S', L')J' \rangle \right|^2 \quad ...(1)$$

where A (aJ; bJ') is the emission rate for the electronic transition from state a of J to the state b of J′, ν is the energy of the transition in cm^{-1}, h the Planck constant, n the refractive index of the medium, e the electronic charge and Ω_t is the value of Judd-Ofelt parameter respectively for t = 2, 4, and 6. $\left| \langle (S,L)\, J \| U^{(t)} \| (S', L')\, J' \rangle \right|^2$ is the square of the reduced matrix elements of the respective component of the transition.

Fortunately, for $^5D_0 \rightarrow {}^7F_2$ electric dipole transition of Eu^{+3}, only Ω_2 is active, so the expression given in Eq. (1) in this case becomes simpler. We have used the value n for pure[22] Y_2O_3 = 1.92 and Ω_2 for $^5D_0 \rightarrow {}^7F_2$ electric dipole transition of Eu^{+3} in pure[23] $Y_2O_3 = 6.31\times10^{-20}$ cm^2 to calculate the emission rate of the pure Y_2O_3:Eu^{+3}. In case of the (Al^{+3}, B^{+3}) containing sample, we assumed that the presence of trace amount of impurity in the Y_2O_3 does not make any significant change in the refractive index (n) of the medium. The value of the squared reduced matrix element $\left| \langle (S, L)\, J \| U^{(2)} \| (S', L')\, J' \rangle \right|^2$ for the $^5D_0 \rightarrow {}^7F_2$ luminescence transition of Eu^{+3} (0.0039) is taken from Kaminskii[24]. Such calculation yields a value of the Ω'_2 for the (Al^{+3}, B^{+3}) containing sample = 11.06×10^{-20} cm^2, which is significantly higher than that of Eu^{+3} in pure Y_2O_3 ($\Omega_2 = 6.31\times10^{-20}$ cm^2). It is also possible to have theoretically an estimate of the ratio of the integrated emission of the $^5D_0 \rightarrow {}^7F_2$ luminescence of a hypothetical Y_2O_3:Eu^{+3} sample where all the Eu^{+3} sites have (Al^{+3}, B^{+3}) as nearest neighbours, to that of the pure Y_2O_3:Eu^{+3}, using the expression in Eq. (2).

$$\text{Integrated emission} = \rho * 8\Pi^3(\nu)^3 e^2/3h(2J+1)*(n^2+2)^2/ \times 9n\, [\Omega_2 \left| \langle (S,L)J \| U^{(2)} \| (S', L')J' \rangle \right|^2] \quad \ldots (2)$$

where ρ represents the concentration of the activator ion (number of ions per cm^3) and the other terms have the usual meanings. Since we have used the same percentage (gram ion) of europium in case of both the samples, we consider that the concentration ρ i.e. number of Eu^{+3} ions per cm^3 is the same for both the pure Y_2O_3:Eu^{+3} and the hypothetical impure sample where all the Eu^{+3} sites have (Al^{+3}, B^{+3}) as nearest neighbours. The calculated results suggest that the (Al^{+3}, B^{+3}) containing hypothetical sample should have integrated emission 1.75 times higher than that of the pure sample. All the experimental and calculated data are presented in Table 1. Ratio of the experimental integrated emission of the actual (Al^{+3}, B^{+3}) containing sample (3738.33 au) to that of the pure sample (2920.76 au), gives a value ~ 1.28, which is some what less than the theoretically predicted value. This is due to the fact that in case of the actual (Al^{+3}, B^{+3}) containing sample, only a small fraction of Eu^{+3} ions has (Al^{+3}/B^{+3}) or both as the nearest neighbours and rest of the Eu^{+3} ions have crystal field similar to that in pure yttria

3.2 Effect of reduction of particle size

In case of this study also, the cubic phase purity of the samples was checked by X-ray diffraction study.

Table 1 — Comparative parameters of luminescence kinetics of Eu^{+3} in pure and (Al^{+3}, B^{+3}) doped Y_2O_3

Phosphor samples	Observed luminescence decay-time $^5D_0 \rightarrow {}^7F_2$ transition	Growth Period of the $^5D_0$ of Eu^{+3}	Judd-Ofelt parameter Ω_2 (cm^2)	Ratio of calculated integrated luminescence. (Impure/pure)	Observed ratio of integrated luminescence (Impure/pure)
Y_2O_3:Eu^{+3}	T =1.07 ×10^{-3} s	152×0^{-6} s	6.31×10^{-20}	1.75	1.28
Y_2O_3:Eu^{+3} Co- doped with Al^{+3}, B^{+3} ions	Biexponential T_1= 0.61×10^{-3} s T_2= 1.05×10^{-3} s	80×0^{-6} s	11.06×10^{-20}		

The crystallite sizes of the samples were calculated from the line width of the principal diffraction line (222) of their respective spectra using the Scherer's equation and also cross checked from their Field Emission Scanning Electron Micrographs (FESEM). The micrograph of the 52 nm nanocrystalline sample is shown as an example in Fig. 5. The $^5D_0 \rightarrow {}^7F_2$ red luminescence efficiencies of the 52 nm nanocrystalline phosphor at its freshly prepared stage and the changes of the same at different stages of ageing are shown in Fig. 6. It is clear from the spectra that the efficiency decreases with the time of ageing. Similar phenonmenon of loss of luminescence efficiency with the time of ageing observed in case of samples of relatively larger particle size, are shown in the Inset of Fig. 6. It is clear from the plot that while the 52 nm samples loses its luminescence intensity from 160 to 80, in 130 day period, the loss in the case of 91 nm sample during the same period is from148 to 140 only. The loss rate is still slower in case of 300 nm sample. The 130 days aged sample of 52 nm size, was heat-treated at 500°C for two hour and then its quantitative luminescence efficiency was checked. The sample was found to regain almost its original luminescence efficiency after heat treatment. It is interesting to note that the rate of loss of luminescence efficiency is the fastest in case of 52 nm sample.

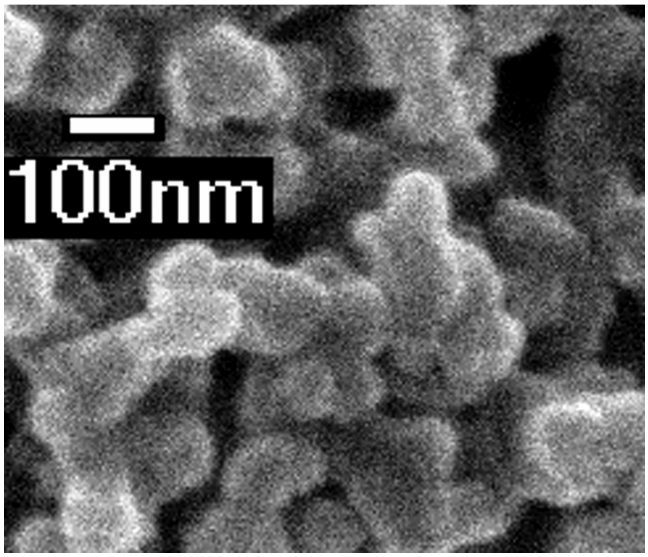

Fig. 5 — FESEM of the Y_2O_3:Eu^{+3} nanophosphor (crystallite size ~ 52 nm)

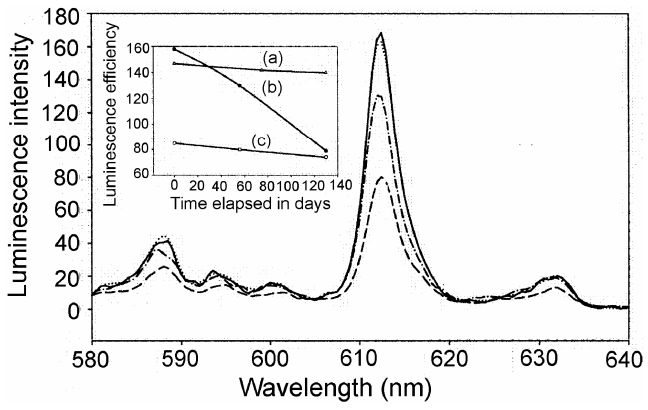

Fig. 6 — Change of luminescence intensity of the Y_2O_3:Eu^{+3} nanophosphor (crystallite size 52 nm) at different stages of ageing: (——) as prepared, (.-.-.-.-) after 56 days, (- - -) after 130 days, (…..) after heat treatment. Inset: Plot of loss of luminescence efficiency of the phosphor of different crystallite as a function of time:(a) 52 nm sample, (b) 91nm sample and (c) 300 nm sample

Figure 7 shows the excitation spectra of the red emission of the 52 nm sample at its freshly prepared stage and at different stages of its ageing. A gradual change in the intensity of the excitation spectrum as well as its spectral profile is observed with ageing. Both the effects are most pronounced in case of the Y_2O_3-excitonic band (~ 210 nm) of the spectra. It can be noted that with the ageing the 212 nm (47100 cm^{-1}) host's excitonic band gradually disappears and a number of phonon side bands at around 210.5 nm (47500 cm^{-1}) and 214 nm (46700 cm^{-1}) appear in the spectrum. Another notable phenomenon is that the new vibronic bands appearing in the excitation spectrum due to ageing vanish when the sample is heat treated in air at 500°C for 2 h. A calculation of the energy of separation between the

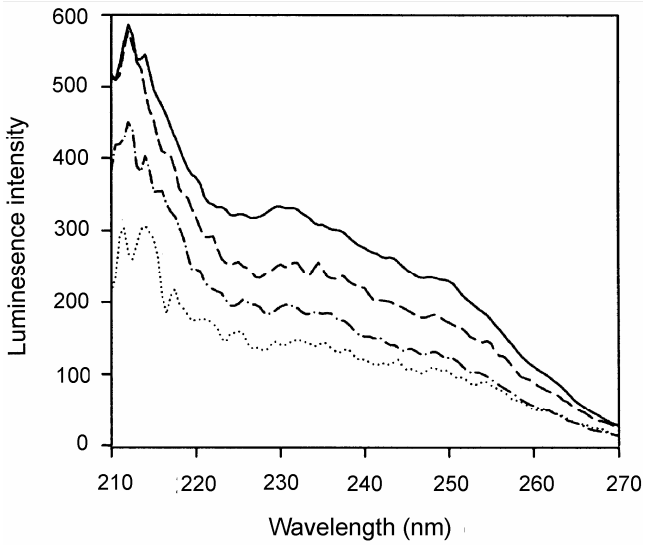

Fig. 7 — Excitation spectra of the 612 nm red luminescence of the 52nm nanophosphor at different stages of its ageing: (——) as prepared, (- - - -) after 56 days, (……) after 130 days, (-.-.-.-) after heat treatment

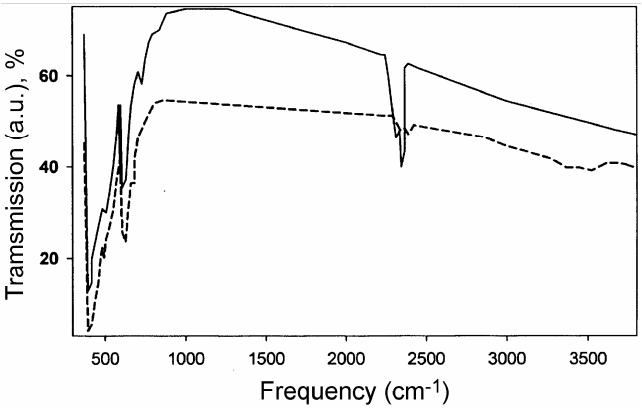

Fig. 8 — IR spectrum of the Y_2O_3:Eu^{+3} 52 nm nanophosphor, (- - -) after ageing; (——), at the freshly prepared stage / after heat treatment

vibronic bands of the 52 nm aged sample gives a value of ~ 400 cm^{-1} or some of its multiple.

IR spectra of the freshly prepared samples as well as after their ageing were also studied. Such IR spectrum of the 52 nm sample is shown in Fig. 8. The spectrum of the sample at its freshly prepared stage exhibits a set of bands at around 390, 417, 467 and 561 cm^{-1}, due to different phonon modes of Y_2O_3. No other bands excepting a band around 2365 cm^{-1} due to the asymmetric stretching mode of CO_2 was observed in the higher frequency region. The spectrum, recorded after ageing of the sample, exhibited additional bands in the frequency region 2000-4000 cm^{-1} e.g. a broad band showing peaks around 3450 cm^{-1} and 3700 cm^{-1}. This is observed in case of all the samples. Considering the energy of the 3700 cm^{-1} band, we identified it as the asymmetric vibration mode of a water molecular while that of the 3450 cm^{-1} band matches well with the energy of the intermolecularly hydrogen bonded stretching mode of an OH group of the water. The two relatively high frequency bands (3450 cm^{-1} and 3700 cm^{-1}) disappear when the aged samples are heat treated at 500°C for two hours. The phenomenon of disappearance of the above mentioned two bands upon heat treatment also supports the view that the bands are associated with water.

All the samples regain almost their original luminescence efficiency as well as the excitation profile after heat treatment. The result suggest that the phosphor samples absorb water molecules from air during storing and it is the absorbed water which reduces the luminescence efficiency as well as changes the excitation profile of Y_2O_3:Eu^{+3} nanophosphor.

IR spectrum of pure cubic yttrium oxide shows bands above 300 cm^{-1} due to the oxygen motions and deformation of YO_6 octahedra[25-27]. The energy of separation of 400 cm^{-1} between the observed vibronic side bands of the excitation spectrum, energetically matches well with that of the IR sensitive 417 cm^{-1} F_u mode[26] of Y_2O_3. This F_u mode has potential energy distribution[26] like ($12d_1$+ $10d_3$+ $44d_4$+ $8d_{34}$+ $2l_\gamma$). Where d_1 represents the stretching mode of Y–O bonds of the S_6 site, d_3 and d_4 represent the stretching mode of Y–O bonds of the C_2 site and γ represents the O–Y–O angle-bending mode of the cubic Y_2O_3. Considering the distribution profile of the potential energy distribution of the F_u mode, it is logical to argue that the contribution of different Y–O stretching modes corresponding to the C_2 site dominates in the Fu mode of Y_2O_3. It has already been established from XPS study[28] of cubic Y_2O_3 that the Y–O bonds of the C_2 site are less covalent than that of the bonds in the S_6 site; and hence, Y–O bond distance of the C_2 site is relatively larger. The oxygen atom of such a bond may have some partial ionic character and hence,a tendency to form hydrogen bond with a water molecule if the material is kept in contact with water/moisture. It is, therefore, most likely that on storing in air; the phosphor absorbs water from air mainly through formation of hydrogen bond with the oxygen atoms of the Y–O bonds of the C_2 sites. The appearance of the 3450 cm^{-1} band in the IR spectrum which is known to arise from an intermolecularly hydrogen bonded OH stretching mode of a water molecule, supports the above view. Such hydrogen-bonded water molecules possibly help the 417 cm^{-1} Fu mode of Y_2O_3 to get coupled with the excitonic transition state of the latter, and activate new vibronic modes to take part in the deactivation process of the phosphor. Since the possibility of hydration increases as the crystallite size of the phosphor decreases due to the obvious reason of increase in the surface to volume ratio, a sample of particle size of few nanometers takes very little time to get effectively hydrated while particles of relatively higher sizes require more time for the same. However, a sample of higher crystallite size (e.g.1 micron or above) can never be able to reach the level of hydration of a nanophosphor what ever may be the time of storage because of their lower values of surface to volume ratios. Thus, a nanophosphor at the freshly prepared stage, because of its relatively larger surface area and

consequently more effective excitation, may exhibit an enhancement of luminescence efficiency compared to that of a micron size counter part; but with the elapse of time, as hydration progresses, its efficiency decreases because of greater nonradiative loss.

Acknowledgement

The authors gratefully acknowledge the financial support from CSIR, India, under the task force project (CTSM) for this work.

References

1 Kotera Y, Higashi T, Sugai M & Ueno A, *J Lumin*, 31, 32 (1984) 709.
2 Van Schaik W & Blasse G, *Chem Matter*, 4 (1992) 410 .
3 Tao Y, Zhao G, Zhang W & Xia S, *Mater Res Bull*, 32 (1997) 501 .
4 Tissue B M, *Chem Mater*, 10 (1998) 2837.
5 Sharma P K, Jilavi M H, Nass R & Chmidt S H, *J Lumin*, 82 (1999) 1876
6 Wakefield G, Holland E, Dobson P J & Hutchison J L, *Adv Mater*, 13 (2001) 1557.
7 Yi S-S, Bae J S, Moon B K, Jeon J H, Park J-C & Kim I W, *Appl Phys Lett*, 81 (2002) 3344 .
8 Sahoo R, Bhattacharya S K & Debnath R, *J Mater Res*, 18 (2003) 609.
9 Chong M K, Pita K & Kam C H, *Appl Phys A*, 79 (2004) 433.
10 Igarashi T, Ihara M, Kusunoki T & Ohno K, *Appl Phys Lett*, 76 (2000) 1549.
11 Dhanaraj J, Jagannathan R, Kutty T R N & Lu C H, *J Phys Chem B*, 105 (2001) 11098.
12 Song H, Wang J, Chen B, Peng H & Lu S, *Chem Phys Lett*, 378 (2003) 1.
13 Jia C-J, Sun L-D, Luo F, Jiang X-C, Wei L-H & Yan C-H, *Appl Phys Lett*, 84 (2004) 5305.
14 Jia M, Zhang J, Lu S, Sun J, Luo Y, Ren X, Song H & Wang X, *Chem Phys Lett,* 407 (2005) 124.
15 Jung K Y, Lee C H & Kang Y C, *Mater Lett*, 59 (2005)2451.
16 Nayak A, Sahoo R & Debnath R, *J Mater Res*, 22 (2007)35.
17 Debnath R, Nayak A & Ghosh A, *Chem Phys Lett*, 444 (2007) 324.
18 Pauling L & Sappel M D, *Z Crystallogr*, 75 (1930) 128; *JCPDS powder diffraction data* file No 25, 1200.
19 Judd B R, *Phys Rev*, 127 (1962) 750.
20 Ofelt G S, *J Chem Phys*, 37 (1962) 511.
21 Peacock R D, *Structure and Bonding*, 22(1975) 83.
22 *Lange's Handbook of Chemistry* (McGraw Hill Book Company, New York) 1973, 23 Caird J A, Ph D Thesis, University of South California, USA, 1975
23 Kaminskii A, *Laser Crystal; Their physics and properties* (Springer Verlag, Berlin), 1990, p158.
24 Schaak G & Koningstein J A, *J Opt Soc Am*, 60 (1970) 1110.
25 Jollet F, Noguera C, Thomson N, Thromat N, Gautier M & Durand J P, *Phys Rev B,* 42 (1990) 7587.
26 Repelin Y, Proust C, Husson E & Beny J M, *J Solid State Chem*, 118 (1995) 163.
27 Bloor D & Dean J R, *J Phys C: Solid State Physics*, 5 (1972) 1237.